



# Obrabotka metallov - Metal Working and Material Science

Journal homepage: [http://journals.nstu.ru/obrabotka\\_metallov](http://journals.nstu.ru/obrabotka_metallov)



## Structure and properties of WC-10Co4Cr coatings obtained with high velocity atmospheric plasma spraying

Elena Kornienko<sup>1, a,\*</sup>, Igor Gulyaev<sup>2, b</sup>, Viktor Kuzmin<sup>2, c</sup>, Alexandr Tambovtsev<sup>2, d</sup>, Pavel Tyryshkin<sup>2, e</sup>

<sup>1</sup> Novosibirsk State Technical University, 20 Prospekt K. Marksa, Novosibirsk, 630073, Russian Federation

<sup>2</sup> Khristianovich Institute of Theoretical and Applied Mechanics SB RAS, 4/1 Institutskaya str., Novosibirsk, 630090, Russian Federation

<sup>a</sup>  <https://orcid.org/0000-0002-5874-5422>,  [e.kornienko@corp.nstu.ru](mailto:e.kornienko@corp.nstu.ru), <sup>b</sup>  <https://orcid.org/0000-0001-5186-6793>,  [gulyaev@itam.nsc.ru](mailto:gulyaev@itam.nsc.ru),

<sup>c</sup>  <https://orcid.org/0000-0002-9951-7821>,  [vikuzmin57@mail.ru](mailto:vikuzmin57@mail.ru), <sup>d</sup>  <http://orcid.org/0000-0003-1635-9352>,  [alsetam123@icloud.com](mailto:alsetam123@icloud.com),

<sup>e</sup>  <https://orcid.org/0009-0009-8125-6772>,  [pavel99730@gmail.com](mailto:pavel99730@gmail.com)

### ARTICLE INFO

#### Article history:

Received: 24 March 2023

Revised: 02 April 2023

Accepted: 08 April 2023

Available online: 15 June 2023

#### Keywords:

Plasma spraying  
 High velocity atmospheric plasma spraying  
 Coating  
 WC-Co  
 HV-APS

#### Funding

The work was supported by the Ministry of Science and Higher Education (project No. 121030500145-0).

#### Acknowledgements

Research was partially conducted at core facility "Structure, mechanical and physical properties of materials".

### ABSTRACT

**Introduction.** Carbon steel is often used for the manufacture of various machine parts, but its operation in aggressive conditions (operation of steel parts under conditions of wear, high temperatures and aggressive corrosive environments) contributes to an extreme decline in properties, up to failure. To solve this problem the modification of the working surfaces of steel parts can be used. It increases its wear resistance, corrosion resistance, and service life. Metal-ceramic coatings based on WC are often used to improve the hardness, wear resistance and corrosion resistance of steel parts. The work purpose is to study the effect of high velocity atmospheric plasma spraying (HV-APS) modes on the structure, phase composition and properties of WC-Co coatings. **Materials and methods.** 86% WC-10% Co-4% Cr coatings were deposited on a mild steel substrate with help of the HV-APS method. The structure and phase composition of the coatings were analyzed using optical microscopy, scanning electron microscopy, and X-ray phase analysis. In addition, the results of measurements of porosity, microhardness, wear resistance, as well as a qualitative assessment of the adhesion are shown in this paper. Results and discussion. It is shown that all coatings are characterized by high density, absence of cracks and oxide films. Using the SEM and XRD methods, it is found that the coatings contain WC and W<sub>2</sub>C particles uniformly distributed in the metal matrix. The matrix is an amorphous or nanocrystalline supersaturated Co(W,C) solid solution. The maximum amount of carbides (49 %) is observed in coatings obtained by deposition from a distance of 170 mm, arc current – 140 A; the minimum (25 %) is observed in coatings obtained by deposition from a distance of 250 mm, arc current – 200 A. The coatings with the maximum amount of carbides have the maximum values of microhardness (1,284 HV<sub>0.1</sub>) and wear resistance. It is established that all coatings are characterized by high adhesion.

**For citation:** Kornienko E.E., Gulyaev I.P., Kuzmin V.I., Tambovtsev A.S., Tyryshkin P.A. Structure and properties of WC-10Co4Cr coatings obtained with high velocity atmospheric plasma spraying. *Obrabotka metallov (tehnologiya, oborudovanie, instrumenty) = Metal Working and Material Science*, 2023, vol. 25, no. 2, pp. 81–92. DOI: 10.17212/1994-6309-2023-25.2-81-92. (In Russian).

## Introduction

Various machine components are often made of steel. This is because steel has the complex of high mechanical, technological and physical-chemical properties. Despite these advantages, the operation of steel components in aggressive conditions – operation of steel parts under conditions of wear, high temperatures and aggressive corrosive environments – contributes to a rapid decrease in its properties, up to failure. The

#### \* Corresponding author

Kornienko Elena E., Ph.D. (Engineering), Associate Professor  
 Novosibirsk State Technical University,  
 20 Prospekt K. Marksa,  
 630073, Novosibirsk, Russian Federation  
 Tel.: 8 (383) 346-11-71, e-mail: [e.kornienko@corp.nstu.ru](mailto:e.kornienko@corp.nstu.ru)

solution to this problem is the modification of the working surfaces of steel parts can be used to increase its wear resistance and corrosion resistance, which will increase its service life [1, 2]. In addition, the formation of thin coatings saves a permissible level of ductility of the components.

Steel components with cermet coatings based on tungsten carbide ( $WC$ ) are often used in industries such as oil, aerospace, metallurgical, chemical, and machine building due to its high hardness, wear resistance, and corrosion resistance [3–6]. The main technologies for these materials' production are  $HVOF$  and  $APS$  [7–11]. Due to its high hardness and brittleness,  $WC$  particles are usually deposited together with a metal binder to form composite coatings. Such coatings combine high ductility, impact strength, and technological effectiveness of the binder ( $Co$ ,  $Ni$ ,  $Ti$ ,  $Fe$ ,  $Cu$ , and others) and high wear and corrosion resistance of ceramics [12, 13].

The change the spraying modes or the characteristics of the sprayed powder allows control the structure, phase composition, and also the properties of the coatings. The authors of [14] established the dependence of the porosity and corrosion resistance of 88%  $WC$ -12%  $Co$   $HVOF$  coatings on the heating temperature of particles in a carrier gas jet. A higher heating temperature contributed to the formation of an amorphous structure in the coatings and an increase in corrosion resistance. The authors of [15] showed that the change of  $HVOF$  modes affect the phase composition, porosity, and hardness of 88%  $WC$ -12%  $Co$  coatings and allow controlling its tribological characteristics. It is stated in [16–18] that the use of nanostructured  $WC$ - $Co$  powder makes it possible to significantly increase the hardness, wear resistance, and corrosion resistance compared to coatings obtained from micron-sized  $WC$ - $Co$  powders. The paper [7] shows that the use of pore-free ultrafine-grained  $WC$ - $Co$  powder made it possible to obtain coatings consisting only of  $WC$  and an amorphous and nanocrystalline  $Co$  matrix. Its wear resistance was 4 times higher than that of coatings obtained from a coarser powder. On the other hand, the authors of [19, 20] demonstrated that when deposited by gas-thermal methods, most of the nanosized  $WC$  powder has time to decompose in the spray jet, which, in turn, leads to a decrease in the wear resistance of the formed coatings. The paper [5] shows that the composition of the  $Ar/He$  or  $Ar/H_2$  plasma-forming gas has an influence on wear resistance more than the size of the sprayed particles. For example, the  $Ar/He$  plasma jet (with a lower operating temperature) reduced the degree of decarburization of the  $WC$  particles and thus increases its volume fraction in the coating. Since the coatings sprayed with  $Ar/He$  jet had a higher volume fraction of  $WC$  particles, it was characterized by higher values of hardness, wear resistance, and also toughness. The authors also reported that during  $Ar/He$  plasma spraying with a jet, coatings made of nanosized powder, rather than made of micron powder, had greater wear resistance.

Sum up, the following conclusion can be drawn: nowadays,  $HVOF$  and  $APS$  methods for obtaining cermet coatings have been investigated in sufficient detail. It is shown that after the development of the technology of deposition of a particular powder, it is possible to clearly control the properties of the resulting coatings. This paper presents the results of studying the effect of  $HV$ - $APS$  modes using air as a plasma-forming gas on the structure, phase composition, and properties of  $WC$ - $Co$  coatings.

## Method of experiment

A commercial granulated 86%  $WC$ -10%  $Co$ -4%  $Cr$  powder with a dispersion of 15–38  $\mu m$  was used for the coatings spraying.  $HV$ - $APS$  was performed using an electric arc plasma torch  $PNK-50$  developed by the *Institute of Theoretical and Applied Mechanics of the Siberian Branch of the Russian Academy of Sciences*. Cylindrical substrates for spraying with a diameter of 20 mm and a height of 7.5 mm were prepared from a commercial low carbon *Steel 20* (0.2% C). The cermet coatings were sprayed to the frontal surface of the cylindrical substrates, which was precleared by sandblasting. Table 1 shows  $HV$ - $APS$  modes. The variable parameter was the spraying distance – 170 and 250 mm and the arc current – 140, 170 and 200 A. Air with the addition of 4 vol.% methane was used as the plasma-forming, transporting, and focusing gas.

Samples for structural studies, as well as measurements of microhardness and porosity, were transverse microsections prepared according to the standard method: mechanical grinding using suspensions containing  $Al_2O_3$  particles of various grain sizes (9, 6, 3 and 1  $\mu m$ ) and finishing polishing on cloth using colloidal

Table 1

The modes of *HV-APS*

Spraying distance, mm	Arc current, A	Spraying modes
170	140	170/140
	170	170/170
	200	170/200
250	140	250/140
	170	250/170
	200	250/200

a solution of silicon oxide with a grain size of 0.04  $\mu\text{m}$ . The microstructure of the samples was studied using an *Olympus GX-51* optical microscope (*Olympus*, Japan) equipped with the *OLYMPUS Stream Image Analysis Stream Essentials 1.9.1* software for measuring the porosity of materials, as well as a *Carl Zeiss EVO50 XVP* scanning electron microscope with an *EDS X-Act* microanalyzer. The phase composition was studied using an *ARL X'TRA* X-ray diffractometer in *CuK $\alpha$*  radiation. The diffraction patterns were recorded at the time  $t = 3$  s with a step  $\Delta 2\theta = 0.05^\circ$ . To reveal the phase composition, a layer about 50  $\mu\text{m}$  thick was removed from each sample from the side of the coating. The microhardness of the structural components of the coatings was evaluated on a *Wolpert Group 402MVD* microhardness tester at a load of 100 g [21].

Wear tests were carried out in accordance with *ASTM G65*. The cermet coatings were spraying on steel plates with the size of 25 $\times$ 75 $\times$ 3 mm. The coatings thickness was 300–350  $\mu\text{m}$ . During the test, the abrasive material (electrocorundum) was fed into the friction zone and pressed against the sample by a rotating rubber roller. The sample was pressed against the roller with a lever (a force of 44 N). The rotational speed of the roller was 60 rpm. Based on the results of weighing, the arithmetic mean value of the weight loss was determined.

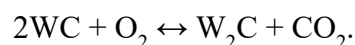
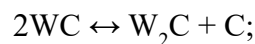
To assess the adhesion of the coatings, the samples were bent with 180° around a guide roll with a diameter of 10 mm according to *ASTM E-290*.

## Results and discussion

### Coatings microstructure

Fig. 1 shows *XRD* spectra of the initial powder and coatings formed by different spraying modes. The main phases of the powder are tungsten carbide *WC* (51-939) and cobalt *Co* (15-806) (Fig. 1, *a*).

The X-ray patterns of all coatings (Fig. 1, *b–g*) are almost the same: the main phases are *WC* (65-4539) and *W<sub>2</sub>C* (35-776). The peak intensity of the *WC* phase in the coatings is lower than in the powder, which indicates its lower volume fraction. It could indicate its lower volume fraction. The *W<sub>2</sub>C* phase is formed as a result of decarburization of *WC* according to the reactions [22]:



The shift of the diffraction peak of the *W<sub>2</sub>C* phase could indicate a change in the interatomic distances.

The absence of cobalt in the coatings' X-ray diffraction patterns is explained with the fact that, during spraying part of the *WC* is dissolved in the cobalt matrix, and then upon rapid cooling an amorphous or nanocrystalline supersaturated *Co(W,C)* solid solution is formed on a cold substrate or already solidified splats. Its formation is indicated by a wide diffraction halo in the range  $2\theta = 37\text{--}47^\circ$ . According to the data of [22–24], the formation of  $\eta$  phases (*Co<sub>3</sub>W<sub>3</sub>C*, *Co<sub>2</sub>W<sub>4</sub>C*, or *Co<sub>6</sub>W<sub>6</sub>C*) is also possible in the matrix, although we did not identify it with X-ray diffraction analysis.

Fig. 2, *a–f* shows the cross-sectional images of the *WC-Co* coatings fabricated by different modes. Its average thickness is 150–200  $\mu\text{m}$ . All coatings are characterized with high density and good adhesion

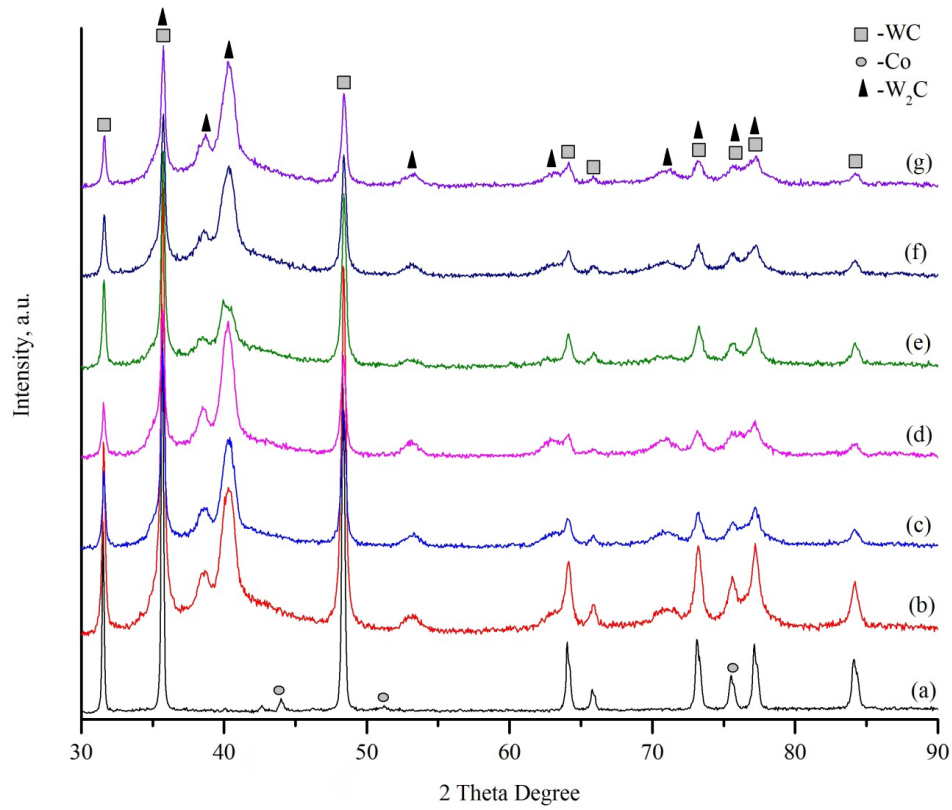
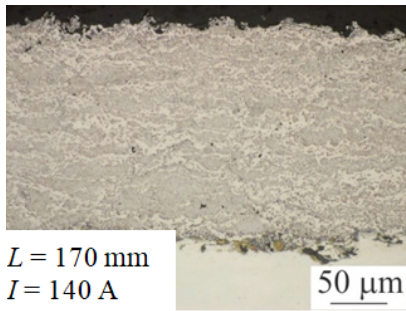
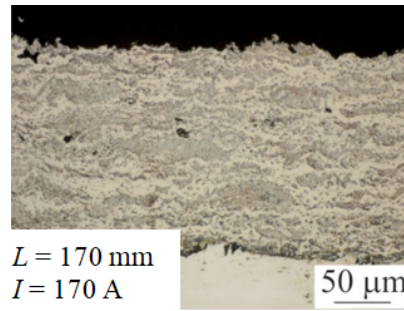


Fig. 1. X-ray diffraction patterns of powder (a) and coatings formed by different modes:

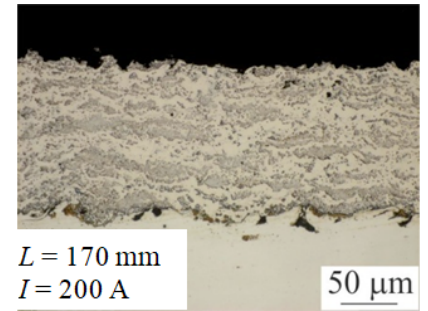
b – 170/140; c – 170/170; d – 170/200; e – 250/140; f – 250/170; g – 250/200



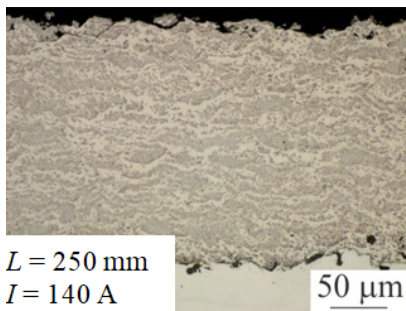
a



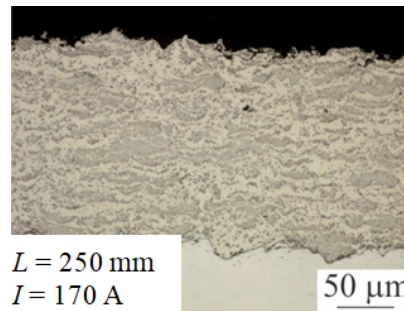
b



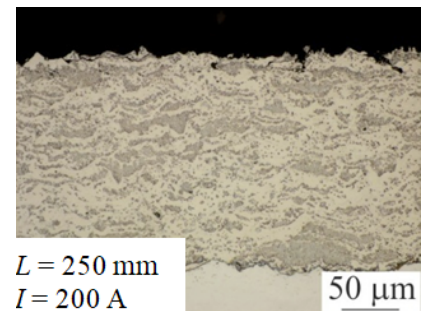
c



d



e



f

Fig. 2. The structure of HV-APS coatings. The modes:

a – 170/140; b – 170/170; c – 170/200; d – 250/140; e – 250/170; f – 250/200

bonding to the substrate. The absence of cracks, as well as carbide particles crumbled out during spraying, indicates a high cohesive bonding. All coatings have a layered structure typical for thermal spraying.

It should be noted that the resulting coatings are characterized by a significant difference in the mass fraction of carbides. Fig. 2, *a–c* (top row) shows coatings obtained at a spraying distance of 170 mm, and Fig. 2, *d–f* (bottom row) – at a distance of 250 mm. The arc current was also changed during spraying: 140 A (Fig. 2, *a, d*), 170 A (Fig. 2, *b, e*) and 200 A (Fig. 2, *c, f*). It can be seen that the spraying distance, as well as the arc current, have a significant effect on the amount of carbides. The dependence of the mass fraction of carbides on the spraying modes is shown in Fig. 3. The amount of  $WC$  and  $W_2C$  decreases with increasing arc current and spraying distance. This is because the arc current increases, therefore the plasma flow temperature also increases, which leads to heating of  $WC$  particles to higher temperatures. The maximum amount of carbides (49 %) is observed in coatings formed using the 170/140 mode, the minimum (25 %) is in the 250/200 mode.

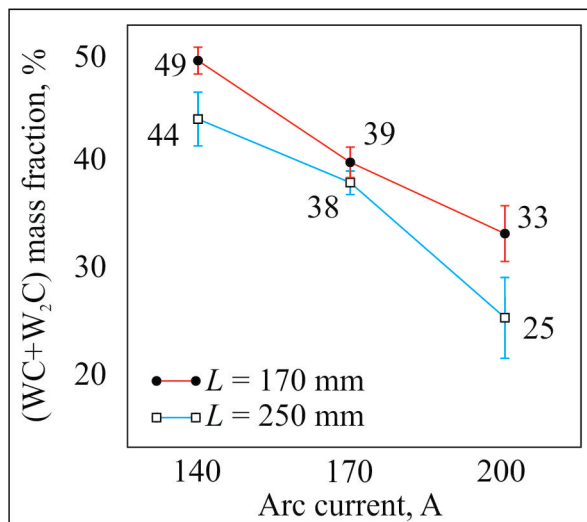


Fig. 3. Dependence of the  $WC+W_2C$  mass fraction on spraying modes

Fig. 4, *a* shows the *SEM* image of the coating obtained by the *BSE* mode. It can be seen that the  $WC$  particles are located inside the splats and have different size (points 4 and 5 in Fig. 4, *a*). There are also areas without  $WC$  particles in the coatings (points 1–3 in Fig. 4, *a*). Depending on the time of exposure to high temperatures on the tungsten carbide particles, the degree of its decomposition will be different. It is known that when heated in a plasma jet,  $WC$  particles begin to melt and tungsten and carbon atoms diffuse into the liquid cobalt matrix. When this molten material is cooled at rates much higher than the critical ones, an amorphous or nanocrystalline supersaturated  $Co(W,C)$  solid solution is fixed. The scheme (Fig. 4*b*) shows that the degree of decarburization of  $WC$  particles is not the same in different splats. Thus, the particles practically do not melt in splats with a darker matrix (point 5 in Fig. 4, *a*) in contrast to splats with a lighter matrix (point 4 in Fig. 4, *a*). Depending on the amount of tungsten and carbon dissolved in cobalt, the matrix is characterized by different shades of gray. According to the X-ray microanalysis data (Table 2), the lighter areas (point 1 in Fig. 4, *a*) contain more tungsten, while the darker areas (point 3 in Fig. 4, *a*) contain less. The obtained data are in good agreement with the data of [5].

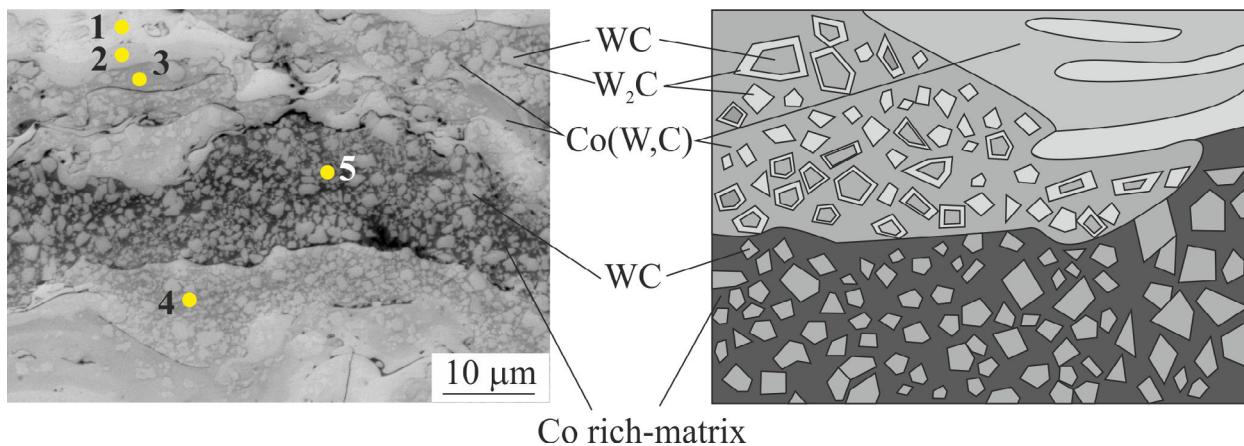


Fig. 4. *SEM* image (*a*) and scheme (*b*) of plasma  $WC-Co$  coating

Table 2

**Electron microprobe analysis of coatings**

Area, No.	Chemical element, wt. %			
	W	Co	C	Cr
1	92.84	2.89	3.52	0.74
2	87.69	3.28	8.23	0.8
3	80.59	7.95	7.45	4.0
4	79.17	9.08	6.83	4.91
5	77.65	10.52	7.87	3.95

**Mechanical properties and wear resistance of WC-Co coatings**

The results of measurements of the coatings microhardness average values depending on the spraying mode are shown in Figs. 5. An increase in the arc current contributes to a decrease in the microhardness values, which can be explained by a decrease in the volume fraction of carbides in the coatings. The influence of the spraying distance is insignificant, while the hardness of the coatings obtained by spraying from a distance of 250 mm is slightly lower. The maximum microhardness (1,284 and 1,287 HV<sub>0.1</sub>) is typical for coatings obtained using the 170/140 and 250/140 modes. The lowest values of microhardness (1,153 and 1,140 HV<sub>0.1</sub>) are specific to coatings obtained using 170/200 and 250/200 modes. On the average, the microhardness of carbides is  $1,432 \pm 107$  HV<sub>0.1</sub>, while that of the cobalt matrix is  $772 \pm 93$  HV<sub>0.1</sub>. The obtained data are in good agreement with the data of [9, 25].

Fig. 6 shows the results of testing coatings for wear with abrasive particles. According the obtained data, the maximum wear resistance is typical for samples with cermet coatings obtained by 170/140 mode (relative wear resistance – 0.21), the minimum wear resistance is characterized for samples obtained by 250/200 mode (relative wear resistance – 0.14). The decrease in wear resistance can be explained by a decrease in the volume fraction of the carbide phase, which is in a good agreement with the results of microhardness measurements.

To evaluate the adhesion of the coatings, 180° bend tests were carried out in the work. In all cases, the coatings cracked in the bending area, but did not peel off. Fig. 7 shows images of the surface of plates with coatings obtained by modes 170/140 (Fig. 7, a) and 250/200 (Fig. 7, b) after testing. It can be seen

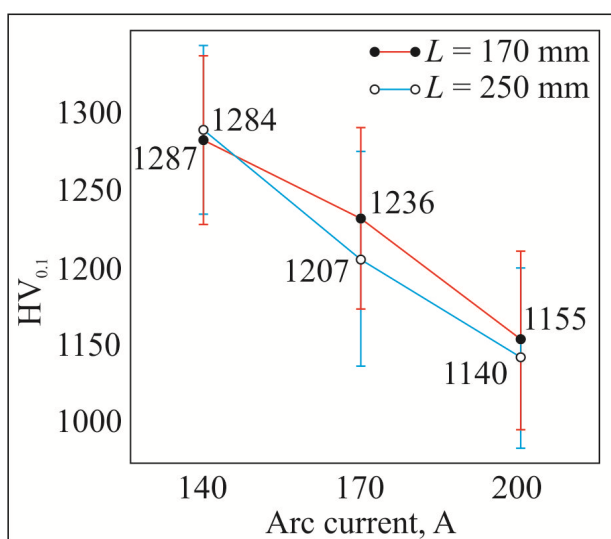


Fig. 5. Microhardness of coatings formed by different modes

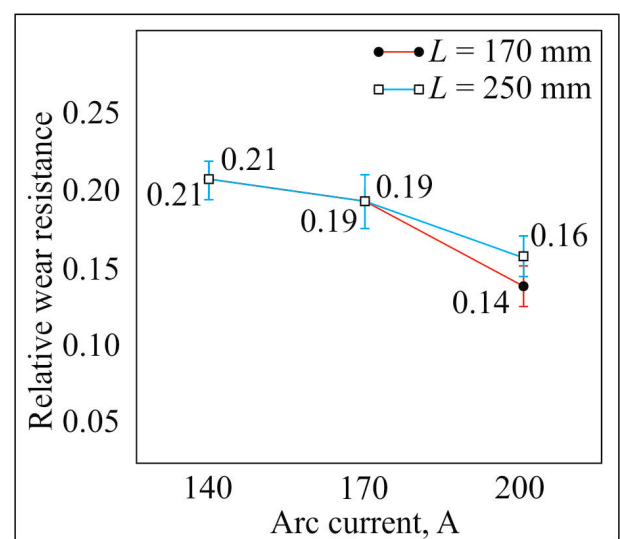


Fig. 6. Relative wear resistance of coatings formed by different modes

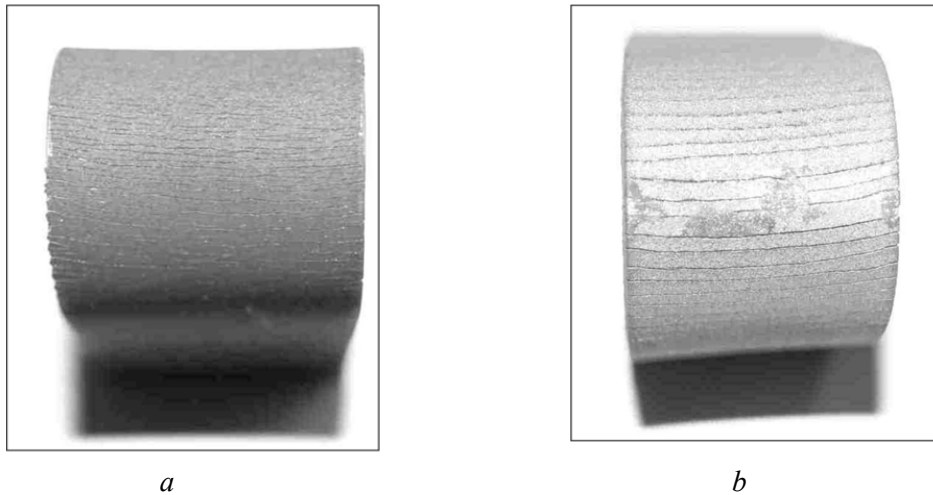


Fig. 7. The specimens with coatings after bend test:  
 a – 170/140; b – 250/200

that the cracks in the coatings are almost straight without any branching. The distance between cracks increases with increasing arc current and spraying distance. The obtained data indicate a high adhesion of the coatings.

### Conclusions

1. In this paper, a range of high-quality  $WC-Co$  coatings were formed with using of  $HV-APS$ . These coatings are characterized by high density, absence of cracks and oxide films.
2. All coatings consist of  $WC$  and  $W_2C$  particles uniformly distributed in the metal matrix. The matrix is an amorphous or nanocrystalline supersaturated  $Co(W,C)$  solid solution.
3. It has been shown that the spraying distance, as well as the arc current, has a significant effect on the volume fraction of carbides. The maximum amount of carbides (49%) is observed in coatings obtained by the 170/140 mode, the minimum ones (25%) — in coatings obtained by the 250/200 mode.
4. The maximum microhardness of coatings is 1,284 and 1,287  $HV_{0.1}$  (modes 170/140 and 250/140), the minimum microhardness is 1,153 and 1,140  $HV_{0.1}$  (modes 170/ 200 and 250/200).
5. The maximum wear resistance is typical for samples with coatings obtained by the 170/140 mode (relative wear resistance 0.21), the minimum value has coatings obtained by the 250/200 mode (relative wear resistance 0.14).
6. All coatings are characterized with high adhesion. It cracked in the bending area, but did not peel off.

### References

1. Afzal M., Ajmal M., Nusair Khan A., Hussain A., Akhter R. Surface modification of air plasma spraying WC-12% Co cermet coating by laser melting technique. *Optics Laser*, 2014, vol. 56, pp. 202–206. DOI: 10.1016/j.optlastec.2013.08.017.
2. Wu Y., Hong S., Zhang J., He Z., Guo W., Wang Q., Li G. Microstructure and cavitation erosion behavior of WC-Co-Cr coating on 1Cr18Ni9Ti stainless steel by HVOF thermal spraying. *International Journal of Refractory Metals and Hard Materials*, 2012, vol. 32, pp. 21–26. DOI: 10.1016/j.ijrmhm.2012.01.002.
3. Venter A.M., Luzin V., Maraisa D., Sacks N., Ogunmuyiwa E.N., Shipway P.H. Interdependence of slurry erosion wear performance and residual stress in WC-12wt%Co and WC-10wt%VC-12wt%Co HVOF coatings. *International Journal Refractory Metals and Hard Materials*, 2020, vol. 87, p. 105101. DOI: 10.1016/j.ijrmhm.2019.105101.
4. Wu X., Guo Z.M., Wang H.B., Song X.Y. Mechanical properties of WC-Co coatings with different decarburization levels. *Rare Metals*, 2014, vol. 33, iss. 3, pp. 313–317. DOI: 10.1007/s12598-014-0257-8.

5. Sanchez E., Bannier E., Salvador M.D., Bonache V., Garcia J.C., Morgiel J., Grzonka J. Microstructure and wear behavior of conventional and nanostructured plasma-sprayed WC-Co coatings. *Journal of Thermal Spray Technology*, 2010, vol. 19, iss. 5, pp. 964–974. DOI: 10.1007/s11666-010-9480-5.
6. Liu S.L., Zheng X.P., Geng G.Q. Influence of nano-WC-12Co powder addition in WC-10Co-4Cr AC-HVAF sprayed coatings on wear and erosion behavior. *Wear*, 2010, vol. 269, iss. 5–6, pp. 362–367. DOI: 10.1016/j.wear.2010.04.019.
7. Wang H., Qiu Q., Gee M., Hou C., Liu X., Song X. Wear resistance enhancement of HVOF-sprayed WC-Co coating by complete densification of starting powder. *Materials and Design*, 2020, vol. 191, p. 108586. DOI: 10.1016/j.matdes.2020.108586.
8. Selvadurai U., Hollingsworth P., Baumann I., Hussong B., Tillmann W., Rausch S., Biermann D. Influence of the handling parameters on residual stresses of HVOF-sprayed WC-12Co coatings. *Surface and Coatings Technology*, 2015, vol. 268, pp. 30–35. DOI: 10.1016/j.surfcoat.2014.11.055.
9. Ghadami F., Sohi M.H., Ghadami S. Effect of bond coat and post-heat treatment on the adhesion of air plasma sprayed WC-Co coatings. *Surface and Coatings Technology*, 2015, vol. 261, pp. 289–294. DOI: 10.1016/j.surfcoat.2014.11.016.
10. Yin B., Zhou H.D., Yi D.L. Microsliding wear behavior of HVOF sprayed conventional and nanostructured WC-12Co coatings at elevated temperatures. *Surface Engineering*, 2010, vol. 26, iss. 6, pp. 469–477. DOI: 10.1179/026708410X12506870724352.
11. Rodriguez M.A., Gil L., Camero S., Frerty N., Santana Y., Caro J. Effects of the dispersion time on the microstructure and wear resistance of WC/Co-CNTs HVOF sprayed coatings. *Surface and Coatings Technology*, 2014, vol. 258, pp. 38–48. DOI: 10.1016/j.surfcoat.2014.10.014.
12. Guo C., Chen J., Zhou J., Zhao J., Wang L., Yu Y., Zhou H. Effects of WC-Ni content on microstructure and wear resistance of laser cladding Ni-based alloys coating. *Surface and Coatings Technology*, 2012, vol. 206, pp. 2064–2071. DOI: 10.1016/j.surfcoat.2011.06.005.
13. Zhang J., Lei J., Gu Z., Tantai F., Tian H., Han J., Fang Y. Effect of WC-12Co content on wear and electrochemical corrosion properties of Ni-Cu/WC-12Co composite coatings deposited by laser cladding. *Surface and Coatings Technology*, 2020, vol. 393, p. 125807. DOI: 10.1016/j.surfcoat.2020.125807.
14. Jalali Azizpour M., Tolouei-Rad M. The effect of spraying temperature on the corrosion and wear behavior of HVOF thermal sprayed WC-Co coatings. *Ceramics International*, 2019, vol. 45, iss. 11, pp. 13934–13941. DOI: 10.1016/j.ceramint.2019.04.091.
15. Sahraoui T., Guessasma S., Ali Jeridane M., Hadji M. HVOF sprayed WC-Co coatings: microstructure, mechanical properties and friction moment prediction. *Materials and Design*, 2010, vol. 31, iss. 3, pp. 1431–1437. DOI: 10.1016/j.matdes.2009.08.037.
16. He J., Schoenung J.M. A review on nanostructured WC-Co coatings. *Surface and Coatings Technology*, 2002, vol. 157, iss. 1, pp. 72–79. DOI: 10.1016/S0257-8972(02)00141-X.
17. Gao P.H., Chen B.Y., Wang W., Jia H., Li J.P., Yang Z., Guo Y.C. Simultaneous increase of friction coefficient and wear resistance through hvof sprayed WC-(nano WC-Co). *Surface and Coatings Technology*, 2019, vol. 363, pp. 379–389. DOI: 10.1016/j.surfcoat.2019.02.042.
18. Ghosh G., Sidpara A., Bandyopadhyay P.P. Understanding the role of surface roughness on the tribological performance and corrosion resistance of WC-Co coating. *Surface and Coatings Technology*, 2019, vol. 378, p. 125080. DOI: 10.1016/j.surfcoat.2019.125080.
19. Dent A.H., Palo S., Sampath S. Examination of the wear properties of HVOF sprayed nanostructured and conventional WC-Co cermets with different binder phase contents. *Journal of Thermal Spray Technology*, 2002, vol. 11 (4), pp. 551–558. DOI: 10.1361/105996302770348691.
20. Baik K.H., Kim J.H., Seong B.G. Improvements in hardness and wear resistance of thermally sprayed WC-Co nanocomposite coatings. *Materials Science and Engineering: A*, 2007, vol. 449–451, pp. 846–849. DOI: 10.1016/j.msea.2006.02.295.
21. Kornienko E., Vyalova A., Shikalov V., Kosarev V., Vidyuk T. Intermetallidnye pokrytiya Al<sub>3</sub>Ti, sformirovannye pri pomoshchi kholodnogo gazodinamicheskogo napyleniya i termicheskoi obrabotki [Al<sub>3</sub>Ti Intermetallic coatings obtained with help gas dynamic cold spray and heat treatment]. *Obrabotka metallov (tekhnologiya, oborudovanie, instrumenty) = Metal Working and Material Science*, 2020, vol. 22, no. 1, pp. 80–89. DOI: 10.17212/1994-6309-2020-22.1-80-89.



22. Zhan Q., Yu L., Ye F., Xue Q., Li H. Quantitative evaluation of the decarburization and microstructure evolution of WC–Co during plasma spraying. *Surface and Coatings Technology*, 2012, vol. 206, pp. 4068–4074. DOI: 10.1016/j.surfcoat.2012.03.091.

23. Yuan J., Zhan Q., Huang J., Ding S., Li H. Decarburization mechanisms of WCeCo during thermal spraying: insights from controlled carbon loss and microstructure characterization. *Materials Chemistry and Physics*, 2013, vol. 142, pp. 165–171. DOI: 10.1016/j.matchemphys.2013.06.052.

24. Katranidis V., Gu S., Cox D.C., Whiting M.J., Kamnis S. FIB-SEM sectioning study of decarburization products in the microstructure of HVOF-sprayed WC-Co coatings. *Journal of Thermal Spray Technology*, 2018, vol. 27, pp. 898–908. DOI: 10.1007/s11666-018-0721-3.

25. Fu D., Xiong H., Wang Q. Microstructure evolution and its effect on the wear performance of HVOF-sprayed conventional WC-Co coating. *Journal of Materials Engineering and Performance*, 2016, vol. 25, pp. 4352–4358. DOI: 10.1007/s11665-016-2278-y.

## Conflicts of Interest

The authors declare no conflict of interest.

© 2023 The Authors. Published by Novosibirsk State Technical University. This is an open access article under the CC BY license (<http://creativecommons.org/licenses/by/4.0>).

